Supplementary Information

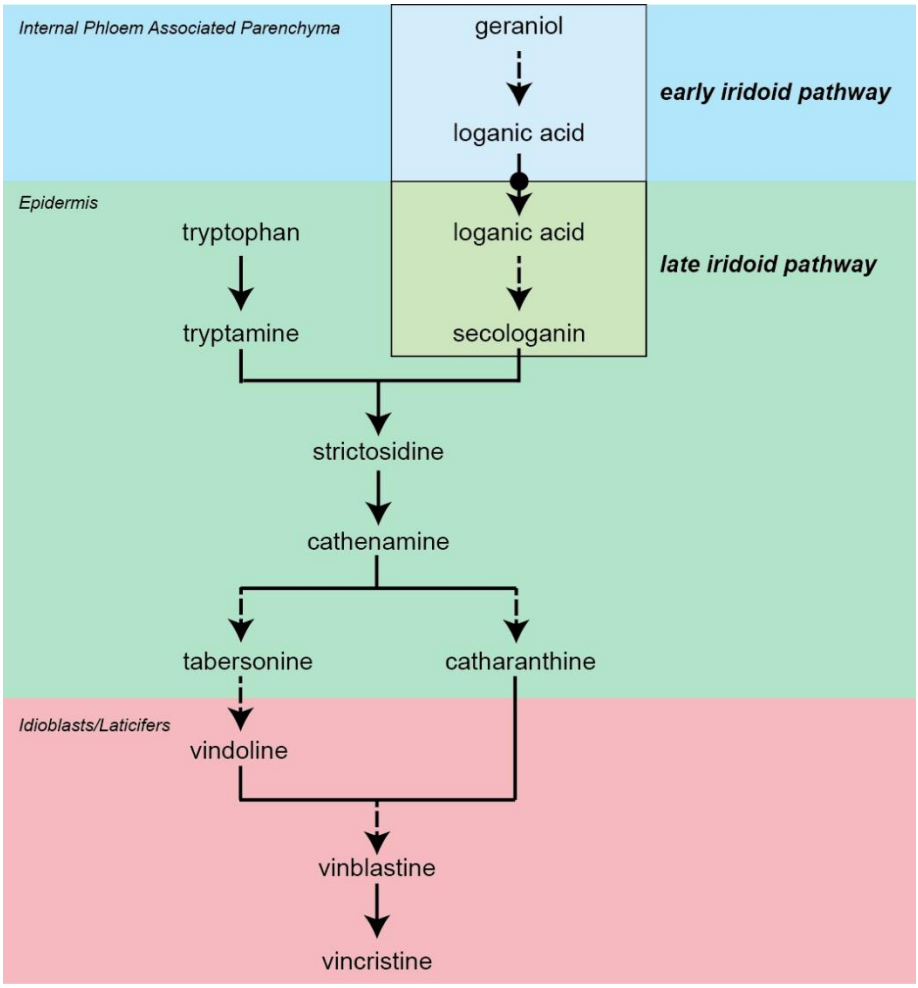

Supplementary Figure 1: Overview of the MIA pathway and the cell-specific localization of the branches leading to vinblastine and vincristine. Solid arrows represent single enzymatic steps, dashed arrows multiple enzymatic steps. The arrow bearing a black circle represents the transport of loganic acid from one type of cells to the other.

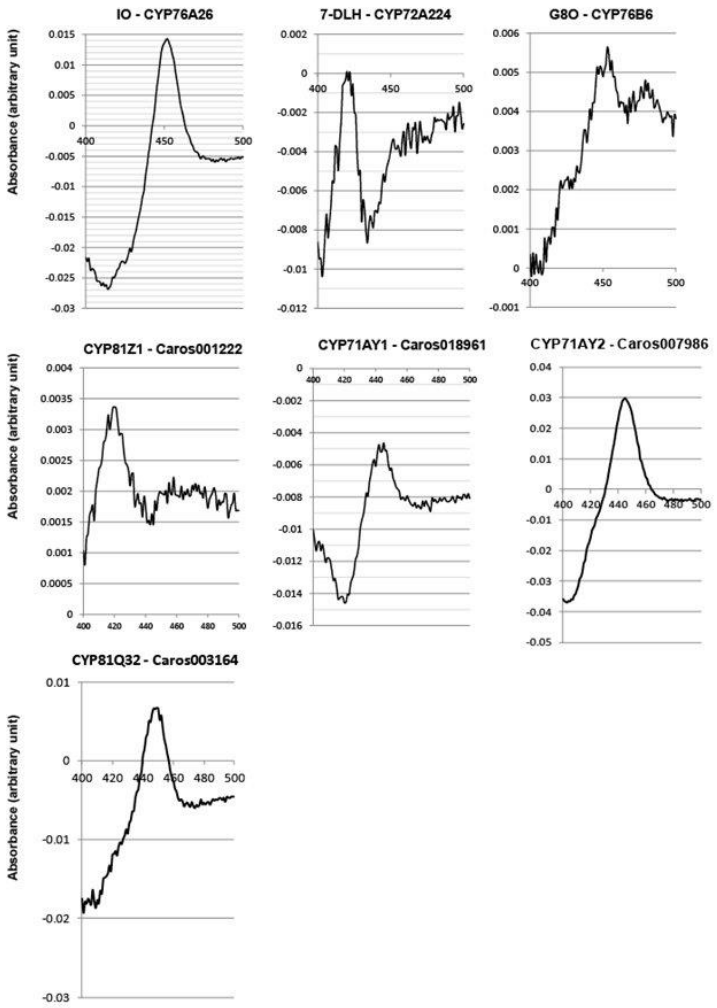

Supplementary Figure 2: Evaluation of the expression of P450 candidates in transformed yeast microsomes. Differential absorbance of the CO-saturated-reduced versus reduced microsomes was recorded between 400 and 500 nm and cytochrome P450 concentration was determined according to [1]. x-axis: wavelength in nm. Iridoid oxidase (IO, CYP76A26, Caros003676), 7-deoxyloganic acid hydroxylase (7-DLH, CYP72A224, Caros005234), Geraniol-8-oxidase (G8O, CYP76B6, Caros006766), CYP81Z1 (Caros001222), CYP71AY1 (Caros018961), CYP71AY2 (Caros007986), CYP81Q32 (Caros003164).

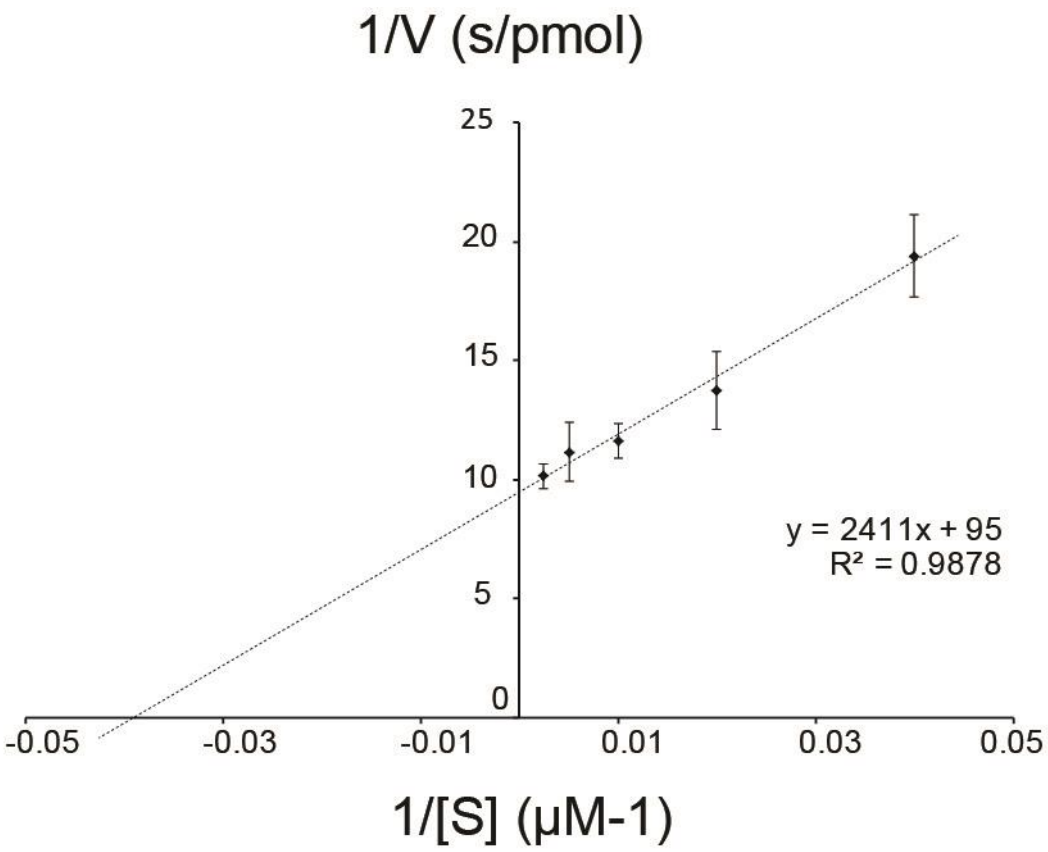

Supplementary Figure 3: Kinetics of the IO reaction. Lineweaver–Burk plot of the reaction rates measured by product formation. The data are means ± standard errors of three replicates.

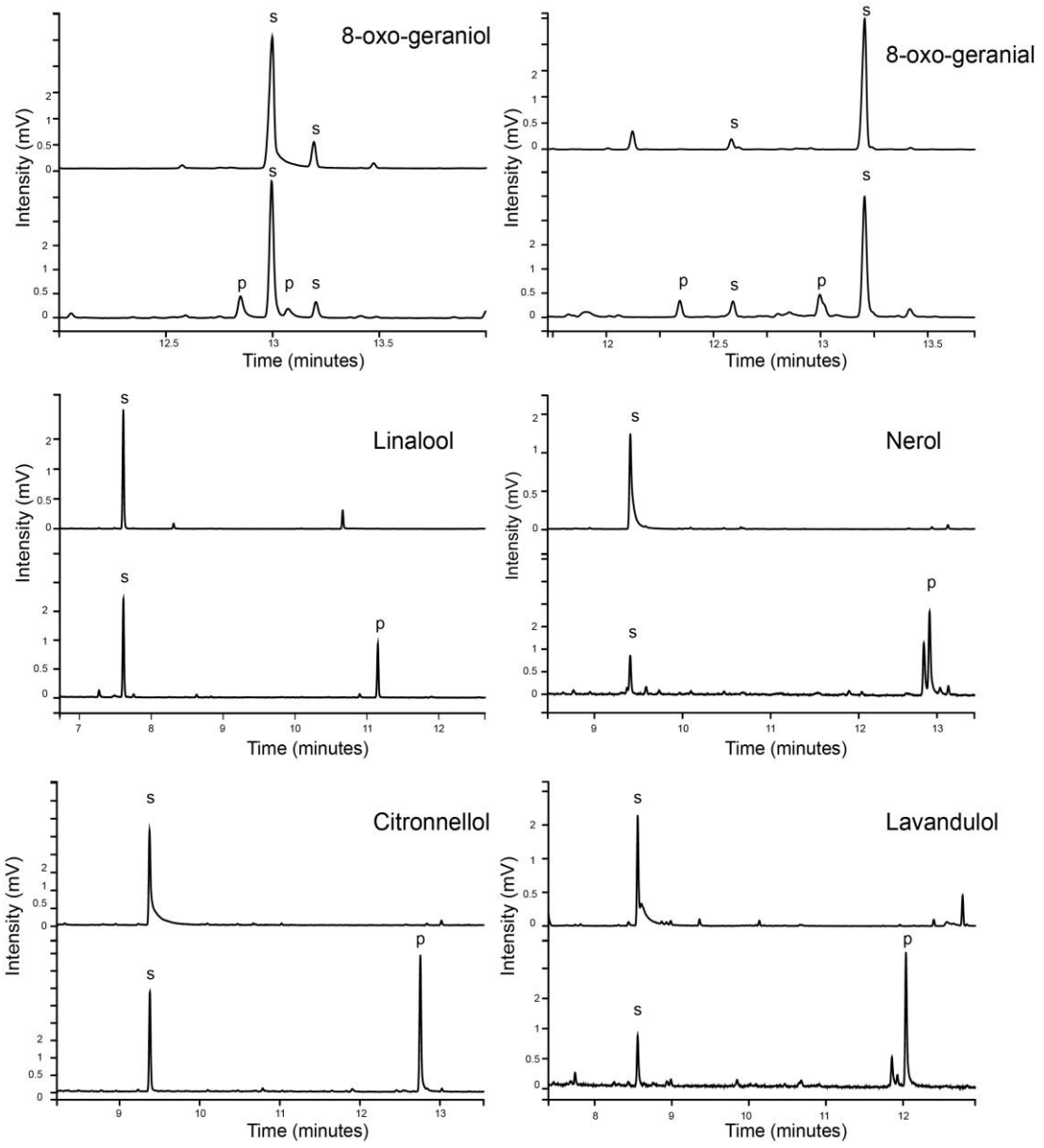

Supplementary Figure 4: Activity of IO with different substrates. Substrates (100 µM) were incubated for 20 min at 27 °C with 23 µM of CYP76A26 (iridoid oxidase, IO) in absence (top) or in presence (bottom) of NADPH. Samples were then extracted with ethyl acetate and analyzed on GC-FID. s: substrate peak(s); p: peak(s) of product(s).

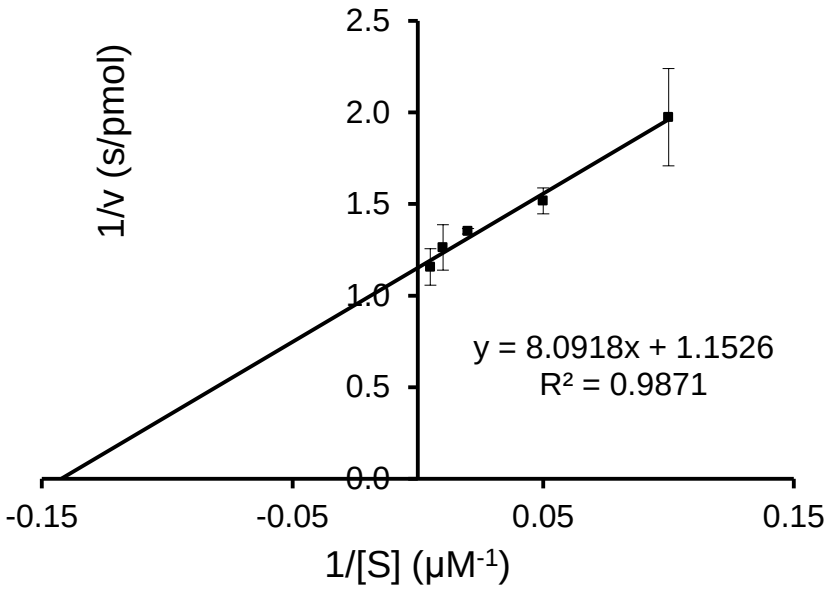

Supplementary Figure 5: Kinetics of the 7-DLGT reaction. Lineweaver–Burk plot of the 7-DLGT reaction rates measured by product formation. The data are means ± standard errors of three replicates.

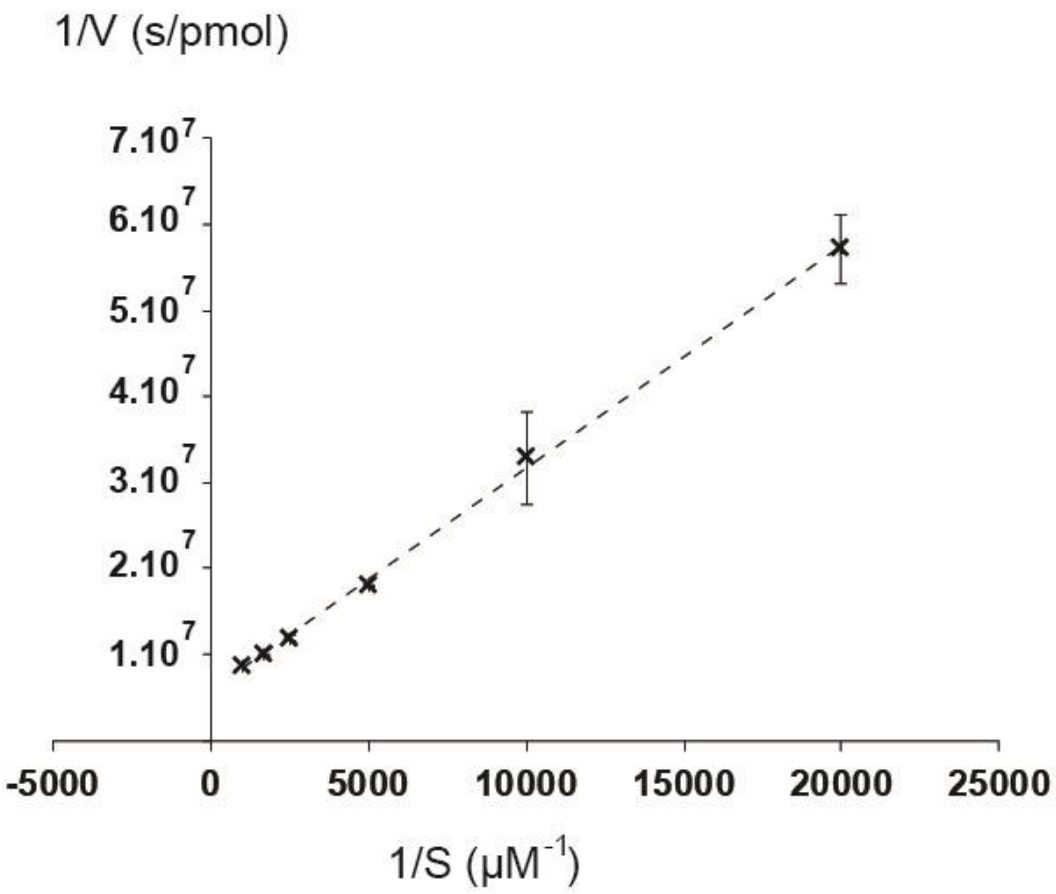

Supplementary Figure 6: Kinetics of 7-DLH reaction. Lineweaver-Burk plot of the 7-DLH reaction rates measured by product formation. The data are means ± standard errors of three replicates.

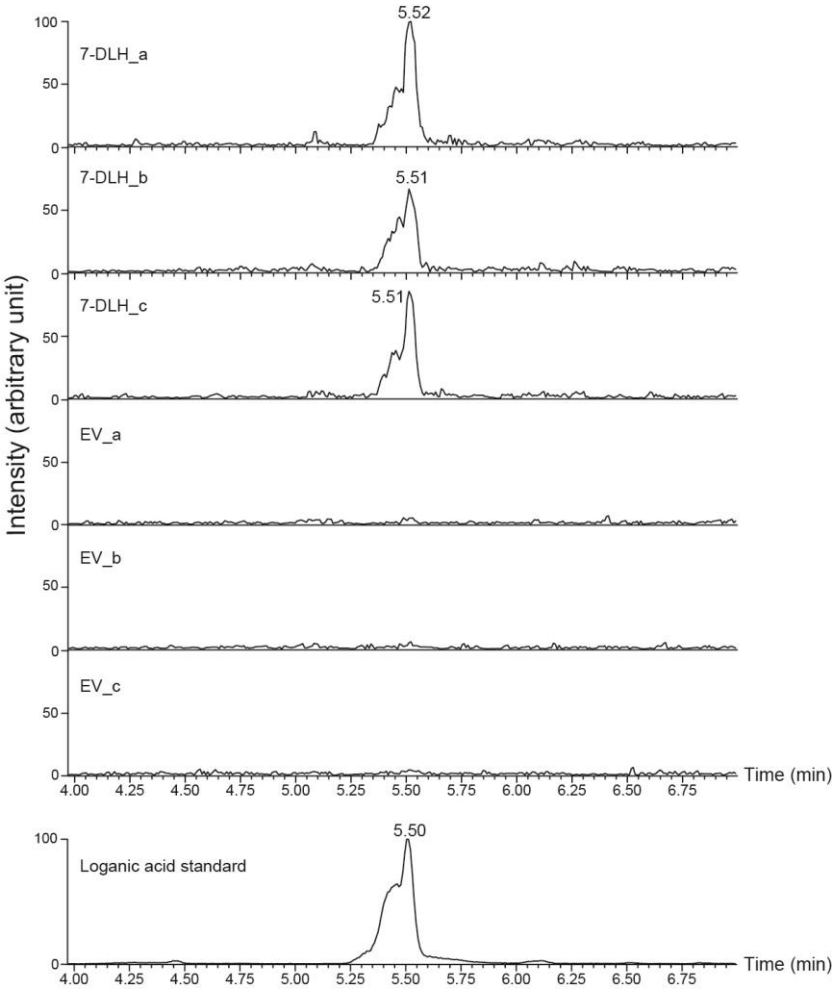

Supplementary Figure 7: Evaluation of 7-deoxyloganic acid conversion into loganic acid by 7-DLH in *N. benthamiana* leaf-disc assay. Discs from leaves agro-infiltrated with a binary vector containing the 7-deoxyloganic acid hydroxylase (7-DLH; CYP72A224) sequence were excised 5 days post-infiltration and incubated for 3 hours on buffer containing 7-deoxyloganic acid. A leaf methanol extract was analyzed on UPLC-MS. Multiple reaction monitoring in positive mode with the transition 215.1>108.9 is shown. EV: extracts of discs agro-transfected with the empty vector incubated with 7-deoxyloganic acid.

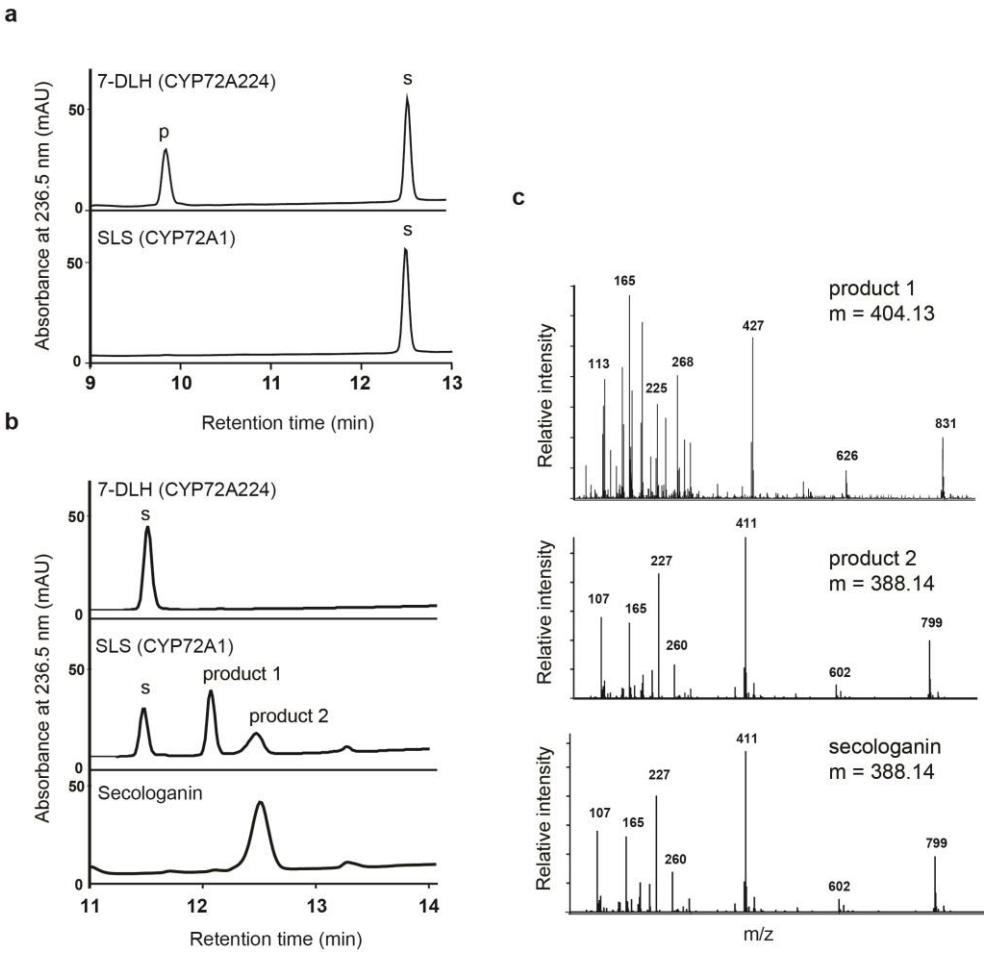

Supplementary Figure 8. Activity of CYP72A224 and CYP72A1 with 7-deoxyloganic acid and loganin. Microsomes from yeast expressing CYP72A224 (7-DLH) or CYP72A1 (SLS) were tested for activity with 7-deoxyloganic acid and loganin. No 7-deoxyloganic acid conversion was observed with SLS (a). No loganin conversion was observed with 7-DLH (b). Identity of the SLS products was determined using MS and authentic secologanin (c). Product 1 corresponds to an oxygenated derivative of secologanin (m = 404.13), product 2 corresponds to reference secologanin (m = 388.14).

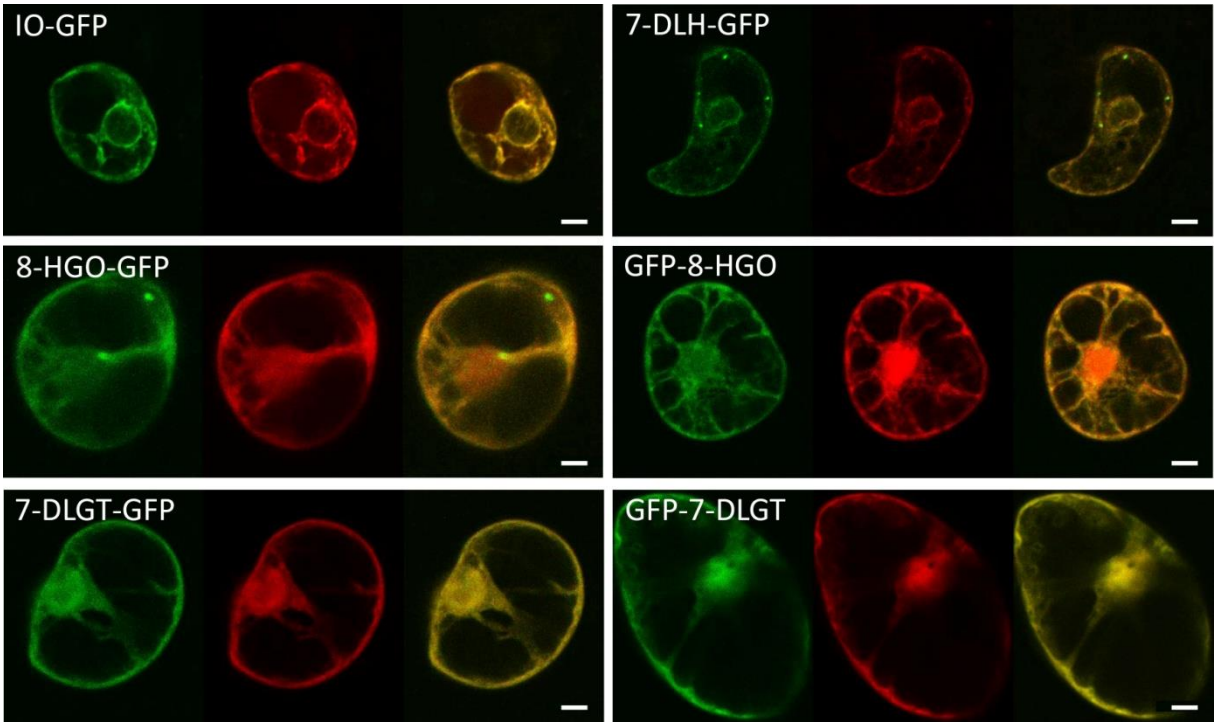

Supplementary Figure 9: Subcellular localization of secoiridoid pathway enzymes. *C. roseus* cells were transiently co-transformed with plasmids expressing pathway enzymes fused to GFP (green; left) and mCherry organelle markers (red; middle). Co-localization of the fluorescent signals appears in the merged pictures in yellow (right). Iridoid oxidase (IO) and 7-deoxyloganic acid hydroxylase (7-DLH) were co-transformed with ER marker and 8-hydroxygeraniol oxidoreductase (8-HGO) and 7-deoxyloganetic acid-*O*-glucosyltransferase (7-DLGT) with cytosol/nucleus marker. Scale bars = 10 µM.

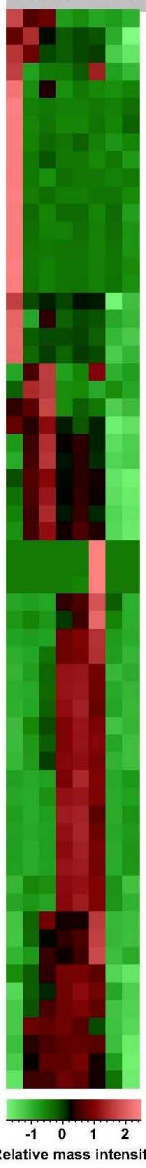

Gene combination 1 2 3 4 5 6 7 8	Retention time	Mass [M $^{-1}$]	Putative identity of basic (geraniol synthase requiring) structure	Putative elemental formula[1]
	18.08	835.3618	geranic acid	2 ($C_{10}H_{16}O_2$+H+F)
	15.18	391.1613	carboxygeraniol (or hydroxygeranic acid)	$C_{10}H_{16}O_3$+H+F
	15.72	377.1823	hydroxygerniol	$C_{10}H_{18}O_2$+H+F
	17.94	699.3267	carboxygeranic acid	$C_{10}H_{14}O_4$+2H+P+F
	27.30	831.3302	geranic acid	2 ($C_{10}H_{16}O_2$+H+M)
	21.36	523.2404	geraniol	$C_{10}H_{18}O$+2H+F
	24.83	375.1673	geranic acid	$C_{10}H_{16}O_2$+H+F
	21.63	477.2341	geraniol	$C_{10}H_{18}O$+2H
	23.22	533.2254	hydroxygerniol	$C_{10}H_{18}O_2$+2H+A
	18.76	685.2920	geraniol	$C_{10}H_{18}O$+3H+F
	27.42	817.3516	NI	$C_{38}H_{58}O_{19}$
	28.14	835.3630	geranic acid	2 ($C_{10}H_{16}O_2$+H+F)
	19.91	725.2859	carboxygeranic acid	$C_{10}H_{14}O_4$+2H+P+2F
	20.95	491.2050	hydroxygerniol	$C_{10}H_{18}O_2$+2H
	27.47	803.3717	geraniol	2 ($C_{10}H_{18}O$+H+M)
	26.43	803.3708	geraniol	2 ($C_{10}H_{18}O$+H+M)
	22.59	493.2297	geraniol	$C_{10}H_{18}O$+H+P+F
	21.46	537.2194	geranic acid	$C_{10}H_{16}O_2$+2H+F
	23.54	519.2459	geraniol	$C_{10}H_{18}O$+2H+A
	20.03	655.2826	geraniol	$C_{10}H_{18}O$+2H+P+F
	18.18	867.3497	carboxygeraniol (or hydroxygeranic acid), one double bond reduced	2 ($C_{10}H_{18}O_3$^{2}+H+M)
	22.11	483.2124	NI	$H_{23}H_{32}O_{11}$
	18.34	657.2047	NI	$C_{29}H_{38}O_{17}$
	15.65	345.1559	carboxygeraniol (or hydroxygeranic acid)	$C_{10}H_{16}O_3$+H
	13.06	521.1876	carboxygeranic acid	$C_{10}H_{14}O_4$+2H
	13.84	521.1952	carboxygeranic acid	$C_{10}H_{14}O_4$+2H
	15.50	359.1356	carboxygeranic acid	$C_{10}H_{14}O_4$+H
	14.70	359.1287	carboxygeranic acid	$C_{10}H_{14}O_4$+H
	12.51	875.2836	carboxygeraniol (or hydroxygeranic acid), two double bond reduced	2 ($C_{10}H_{20}O_3$+H+A+F)
	18.73	659.2226	NI	$C_{29}H_{40}O_{17}$
	17.69	401.1442	7-deoxyloganic acid	$C_{16}H_{24}O_9$+A
	15.12	401.1448	7-deoxyloganic acid	$C_{16}H_{24}O_9$+A
	15.19	359.1371	7-deoxyloganic acid	$C_{16}H_{24}O_9$
	17.33	347.1712	carboxygeraniol (or hydroxygeranic acid), one double bond reduced	$C_{10}H_{18}O_3$+H
	24.18	693.3354	NI	$C_{32}H_{54}O_{16}$
	20.32	391.1978	carboxygeraniol (or hydroxygeranic acid), two double bond reduced	$C_{10}H_{20}O_3$+H+A
	18.20	349.1873	carboxygeraniol (or hydroxygeranic acid), two double bond reduced	$C_{10}H_{20}O_3$+H
	15.38	525.2192	carboxygeranic acid, two double bond reduced	$C_{10}H_{18}O_4$+2H
	17.43	363.1664	carboxygeranic acid, two double bond reduced	$C_{10}H_{18}O_4$+H
	15.77	867.3478	carboxygeraniol (or hydroxygeranic acid), one double bond reduced	2 ($C_{10}H_{18}O_3$+H+M)
	19.46	661.2351	carboxygeraniol (or hydroxygeranic acid), one double bond reduced	$C_{10}H_{18}O_3$+3H
	22.81	499.1826	NI	$C_{23}H_{32}O_{12}$
	17.77	395.1929	carboxygeraniol (or hydroxygeranic acid), two double bond reduced	$C_{10}H_{20}O_3$+H+F
	20.81	843.4240	hydroxygeraniol with two double bond reduced	2 ($C_{10}H_{22}O_2$+H+M)
	17.17	727.3346	carboxygeranic acid, two double bond reduced	2 ($C_{10}H_{18}O_4$+H)
	13.93	673.2944	carboxygeraniol (or hydroxygeranic acid), two double bond reduced	$C_{10}H_{20}O_3$+3H
	20.08	871.3815	carboxygeraniol (or hydroxygeranic acid), one double bond reduced	2 ($C_{10}H_{18}O_3$+H+A+F)
	19.70	187.1347	carboxygeraniol (or hydroxygeranic acid), two double bond reduced	$C_{10}H_{20}O_3$
	15.69	511.2394	carboxygeraniol (or hydroxygeranic acid), two double bond reduced	$C_{10}H_{20}O_3$+2H
	23.34	525.2043	carboxygeranic acid, two double bond reduced	$C_{10}H_{18}O_4$+2H
	24.53	737.3045	NI	$C_{36}H_{50}O_{16}$
	19.55	389.1823	carboxygeraniol (or hydroxygeranic acid), one double bond reduced	$C_{10}H_{18}O_3$+H+A
	14.22	347.1711	carboxygeraniol (or hydroxygeranic acid), one double bond reduced	$C_{10}H_{18}O_3$+H
	16.27	389.1824	carboxygeraniol (or hydroxygeranic acid), one double bond reduced	$C_{10}H_{18}O_3$+H+A
	16.40	393.1768	carboxygeraniol (or hydroxygeranic acid), one double bond reduced	$C_{10}H_{18}O_3$+H+F
	23.54	485.2185	NI	$C_{23}H_{34}O_{11}$
	13.45	361.1513	carboxygeranic acid, two double bond reduced	$C_{10}H_{16}O_4$+H
	26.36	457.2454	NI	$C_{23}H_{38}O_9$
	16.15	361.1510	carboxygeranic acid, two double bond reduced	$C_{10}H_{16}O_4$+H
	21.75	835.3415	NI	$C_{41}H_{56}O_{18}$
	25.01	607.2975	carboxygeraniol (or hydroxygeranic acid), one double bond reduced	$C_{10}H_{16}O_3$+2H+A+F

Supplementary Figure 10. Masses and quantitative changes of compounds detected upon step-wise reconstitution of the secologanin pathway in *N. benthamiana*. Gene combinations are as listed in Fig. 8A. Heatmap shows relative mass intensity changes.[1] F, formic acid adduct; A, acetyl group adduct; M, malonyl group adduct; number 2, dimer; H, hexose, P, pentose. NI : not identified.

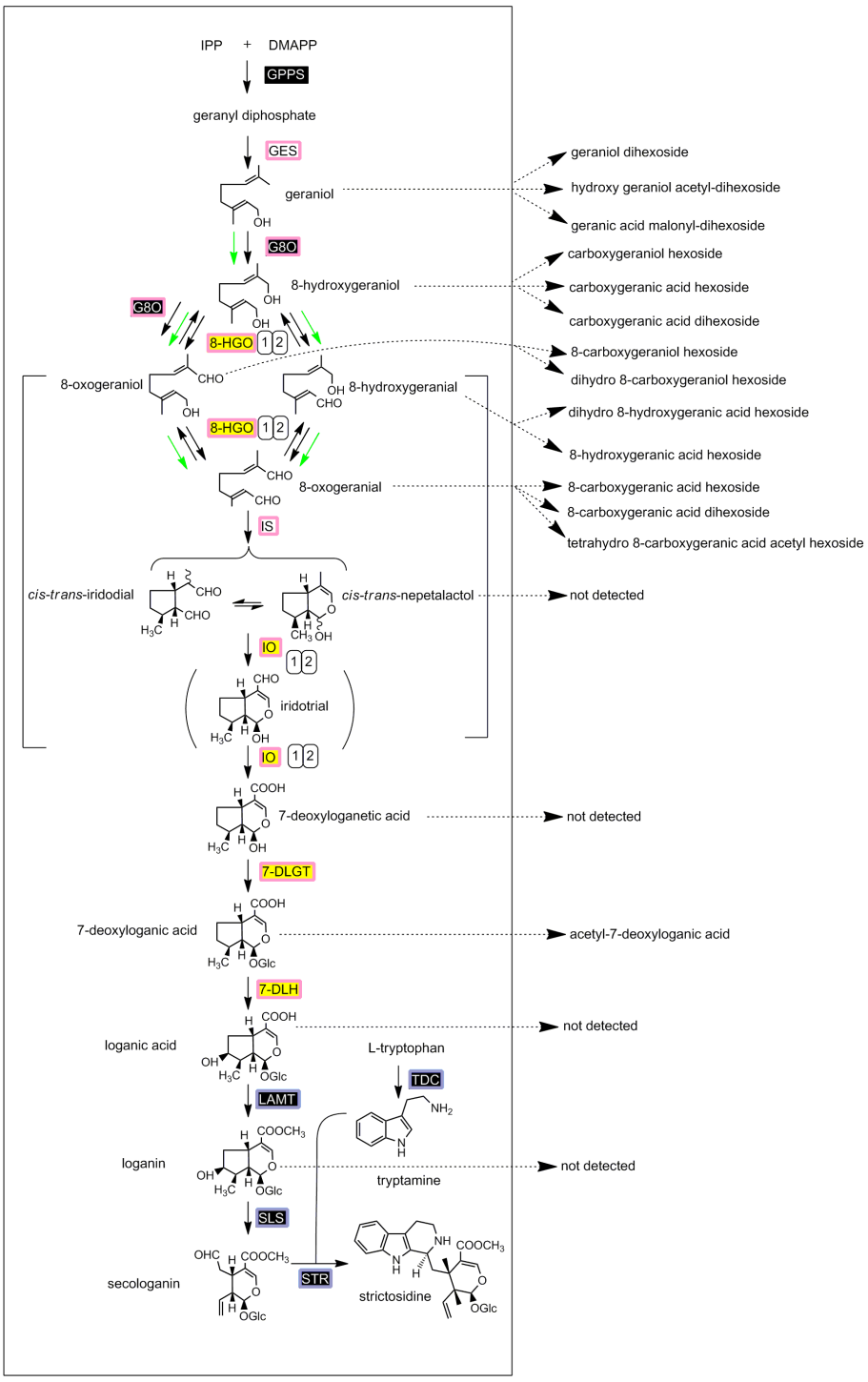

Supplementary Figure 11. Modified pathway intermediates observed in *N. benthamiana*.

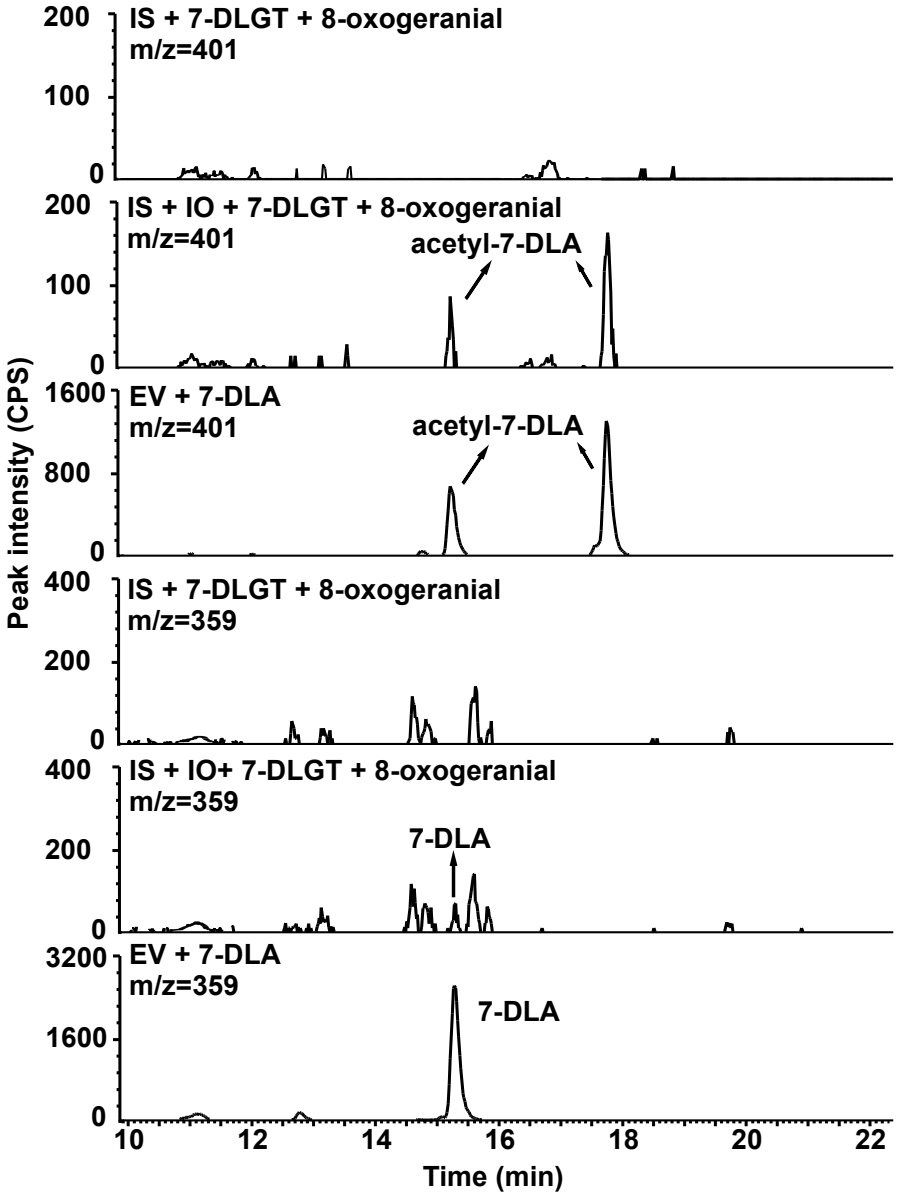

Supplementary Figure 12: Iridoid oxidase is an essential component of the pathway. LC-MS analysis on selected masses 359 (7-deoxyloganic acid; 7-DLA) or 401 (acetylated 7-DLA) of *N. benthamiana* leaves infiltrated with 7-DLA or 8-oxogeranial co- agro-infiltrated with gene combination *IS+IO+7-DLGT,IS+7-DLGT* or empty vector (EV). CPS = counts per second.

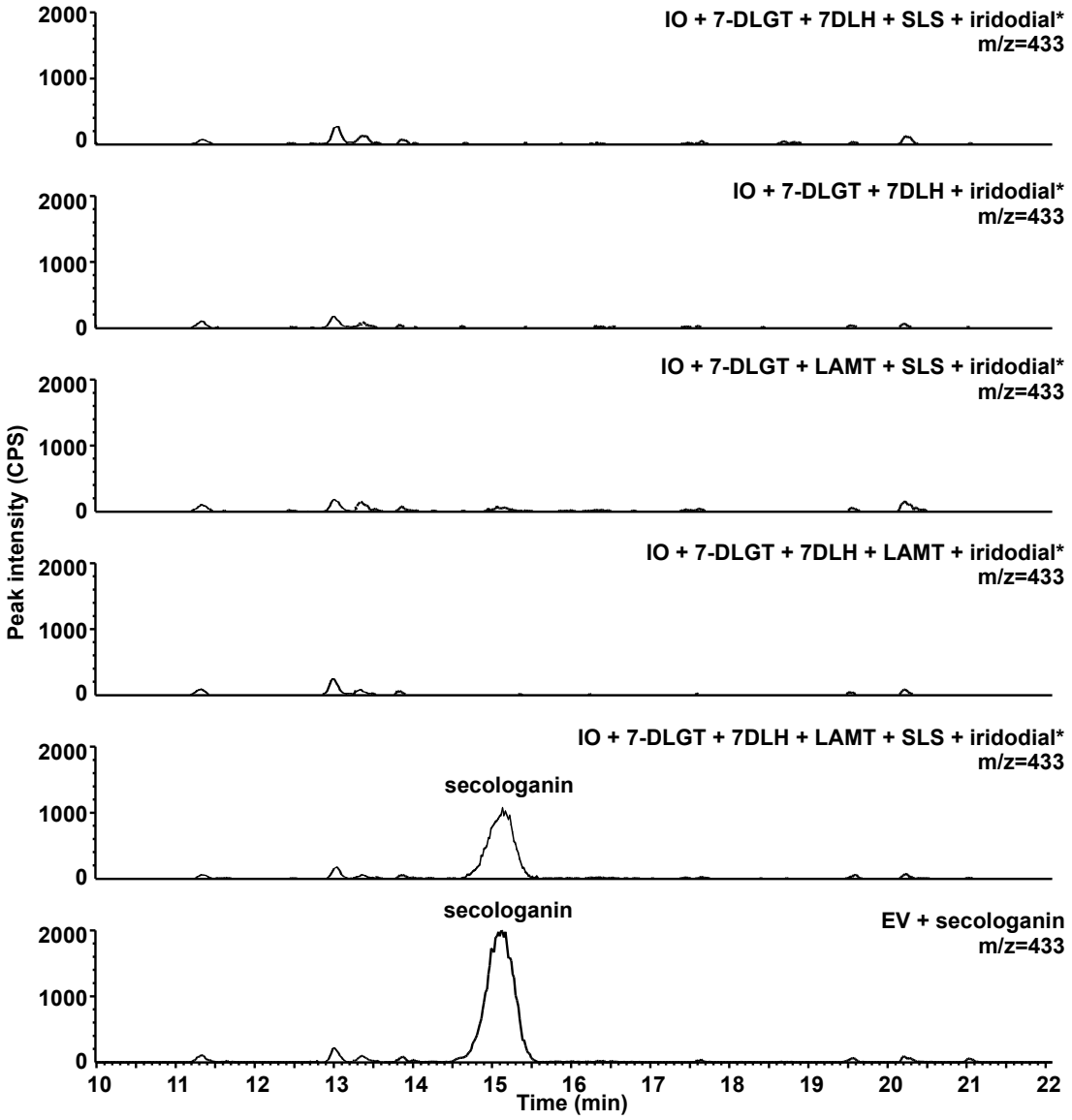

Supplementary Figure 13: Reconstitution of the pathway from iridodial to secologanin in *N. benthamiana*. LC-MS analysis showing selected mass 433 (formic acid adduct of secologanin) of extracts of *N. benthamiana* leaves in which the gene combinations *IO +7-DLGT + 7DLH + SLS, IO + 7-DLGT + 7DLH, IO + 7-DLGT + LAMT + SLS, IO + 7-DLGT + 7DLH + LAMT, IO + 7-DLGT + 7DLH + LAMT + SLS,* or empty vector (EV) were transiently expressed and that were co-infiltrated with iridodial or secologanin as indicated. * indicates that identical profiles were obtained with co-infiltrated iridotrial. CPS = counts per second.

Supplementary Table 1: Candidate enzymes in mesophyll and epidermal cells. A proteomic approach with microsomes isolated from enriched epidermal or mesophyll protoplast fractions was carried out as described in Methods. Shown are candidate enzymes found among 2200 identified proteins and their distribution between mesophyll and epidermis. n.s.: not significant. SD: standard deviation.

Enzyme Class	Enzyme name	proteomics hits					
		Accession number	**Epidermis Mean ± SD**	**Mesophyll Mean ± SD**	**Statistics Fishers exact test Significance level (%)**	**p-value**	**Enrichment**
Cyt P450	CYP72A224	Caros005234	0.0±0.0	2.3±2.5	95	(0.013)	Mesophyll
Cyt P450	CYP76B6	Caros006766	1.0±1.0	14.7±9.9	95	(0.0000000025)	Mesophyll
Cyt P450	CYP81Q32	Caros003164	6.3±4.2	7.7±7.2	0	(0.52)	n.s.
Cyt P450	CYP76A26	Caros020058	0.67±1.2	11.0±8.4	95	(0.00000018)	Mesophyll
Cyt P450	CYP71AY2	Caros007986	8.0±2.6	3.0±2.6	95	(0.0018)	Epidermis
oxidoreductase (alcohol dehydrogenase)	CrADH2	Caros002459	5.3±4.2	0.7±1.2	95	(0.00021)	Epidermis
oxidoreductase (alcohol dehydrogenase)	CrADH3	Caros022489	15.0±10.8	3.3±3.2	95	(0.000000056)	Epidermis
oxidoreductase (alcohol dehydrogenase)	CrADH5	Caros021570	11.7±7.8	4.3±3.2	95	(0.00015)	Epidermis
oxidoreductase (alcohol dehydrogenase)	CrADH8	Caros012730	27.3±17.1	20.0±16.1	95	(0.0036)	Epidermis
oxidoreductase (alcohol dehydrogenase)	CrADH9	Caros017236	16.0±4.6	3.7±6.4	95	(0.000000029)	Epidermis
oxidoreductase (alcohol dehydrogenase)	CrADH11	Caros007544	36.0±6.2	18.7±15.1	95	(0.00000029)	Epidermis
oxidoreductase (alcohol dehydrogenase)	CrADH14	Caros006689	48.0±13.7	11.0±9.5	95	(0.00000000000000000000049)	Epidermis
oxidoreductase (alcohol dehydrogenase)	CrADH15	Caros002170	14.0±5.0	3.0±5.2	95	(0.00000011)	Epidermis
oxidoreductase	CrBBE1	Caros003491	2.0±2.6	0.0±0.0	95	(0.0097)	Epidermis
UGT	CrUGT2	Caros004449	16.3±9.8	5.3±4.5	95	(0.0000015)	Epidermis
UGT	CrUGT3	Caros020739	0.0±0.0	10.3±14.6	95	(0.0000000046)	Mesophyll

Supplementary Table 2: Sequences of primers and cloning methods used for plasmid constructions. Primers are displayed from 5' to 3' end.

Construct	restriction site	primer F	primer R
pRT101 IO	XhoI,KpnI	GGCCTTCTCGAGATGGCGACCATCACTTTCG	AAGGCCGGTACCTTAGATATGAACTCTCTTCTTAGGGATG
pRT101 7-DLH	XhoI,KpnI	GGCCTTCTCGAGATGGAATTGAACTTCAAATCAATTA	GGCCTTGGTACCTTAGAGTTTGTGCAGAATCAAATGAG
pRT101 7-DLGT	KpnI,SpeI	CCGGTACCAATGGGTTCTCAAGAAACAAATTTG	CCACTAGTTCAAATAATCAGTGATTTTATGTAATCAAC
pRT101 8-HGO	KpnI,XbaI	CCGGTACCAATGACCAAGACCAATTCCCCT	GGTCTAGATTAGAACTTGATAACAACTTTGACACAATC
pRT101 CYP81Z1	XhoI,SacI	GGTCTCGAGATGGAGGTTTCCTTTTTCTAC	ACCGAGCTCTTATGGGTTATTTTCCATGG
pRt101 CYp71AY1	XhoI,EcoRI	GGCCTTCTCGAGATGGATCAGCTGATGAACTTCTC	GGCCTTGAATTCTTAGTTTCCTTCAACTACAGTTGAGATG
pRT101 IS	XhoI,KpnI	CCGGTTCTCGAGAATGAGTTGGTGGTGGAAGAGG	CCTTGGGGTACCCTAAGGAATAAACCTATAATCCCTC
pRT101 SLS	XhoI,KpnI	GTTCTCGAGATGGAGATGGATATGGATACCATT	CCGGTACCCTAGCTCTCAAGCTTCTTGTA
pASKIBA45+ 7-DLGT	XhoI,KpnI	CCGGTACCAATGGGTTCTCAAGAAACAAATTTG	GGCTCGAGCAAATAATCAGTGATTTTATGTAATCAAC
pET16H 8-HGO	XhoI, KpnI	CCCTCGAGATGACCAAGACCAATTCCCCT	GGGGTACCTTAGAACTTGATAACAACTTTGACACAATC
pASKIBA45+ IS	XhoI, SalI	CCGGTTCTCGAGAATGAGTTGGTGGTGGAAGAGG	AACCGGGTCGACAAAGGAATAAACCTATAATCCCTC
pET16H IS	XhoI,KpnI	CCGGTTCTCGAGATGAGTTGGTGGTGGAAGAGG	AACCGGGGTACCCTAAGGAATAAACCTATAATCCCTC
pTH2 IO	SalI	CCGTCGACAAAATGGCGACCATCACTTTCG	CCGTCGACGATATGAACTCTCTTCTTAGGGATG
pTH2 7-DLH	SalI	CCGTCGACAAAATGGAATTGAACTTCAAATCAATTA	CCGTCGACGAGTTTGTGCAGAATCAAATGAG
pTH2 7-DLGT	SalI	CCGTCGACAAAATGGGTTCTCAAGAAACAAATTTG	CCGTCGACAATAATCAGTGATTTTATGTAATCAAC
pTH2BN 7-DLGT	XhoI,SpeI	GGCTCGAGATGGGTTCTCAAGAAACAAATTTG	GGACTAGTTCAAATAATCAGTGATTTTATGTAATCAAC
pTH2 8-HGO	SalI	CCGGCCGTCGACAAAATGACCAAGACCAATTCCCCT	CCGGCCGTCGACGAACTTGATAACAACTTTGACACAATC
pTH2BN 8-HGO	XhoI,SpeI	CCGGGGCTCGAGATGACCAAGACCAATTCCCCT	CCGGGGACTAGTTTAGAACTTGATAACAACTTTGACACAATC
pRt101 mCherry	XhoI,KpnI	GGTTCCCTCGAGAAAATGGTGAGCAAGGGCGAGGAGGA	GGCCTTGGTACCTTACTTGTACAGCTCGTCCATGCCGCCGG
pYEDP60 CYP81Z1	USER	GGCTTAAUATGGAGGTTTCCTTTTTCTACAC	GGTTTAAUTTATGGGTTATTTTCCATGGG
pYEDP60 CYP71AY1	USER	GGCTTAAUATGGATCAGCTGATGAACTTCTCTC	GGTTTAAUTTAGTTTCCTTCAACTACAGTTGAGATG
pYEDP60 IO/CrCYP76A26	USER	GGCTTAAUATGGCGACCATCACTTTCTCC	GGTTTAAUTTAGATATGAACTCTCTTCTT
pYEDP60 7-DLH/CrCYP72A224	USER	GGCTTAAUATGGAATTGAACTTCAAATCA	GGTTTAAUTTAGAGTTTGTGCAGAATCAA
pYEDP60 G8H/CrCYP76B6	USER	GGCTTAAUATGGATTACCTTACCATAATATTAAC	GGTTTAAUTTAAAGGGTGCTTGGTACAGC

Supplementary Table 3: Relative conversion rates for 8-HGO substrates.

Values are the average of 4 replicates ± standard error. Compounds were prepared as 100x stock solutions in acetone. Reactions proceeded for 5 min at room temperature with 100 µM of specific substrate, 200 µM NAD^+ and 200 ng enzyme in 50 mM Na-phosphate buffer pH 9. Rates were calculated based on NADH production measured in a spectrophotometer at 340 nm.

Compound	relative conversion rate (%)
8-OH-geraniol	100 ± 11
geraniol	75 ± 8
trans-2-hexenol	72 ± 12
8-oxogeraniol	53 ± 3
farnesol (mix of isomers)	48 ± 7
nerol	43 ± 8
8-OH-geranial	33 ± 4
4-isopropylbenzyl alcohol	29 ± 4
octanol	10 ± 2
3,7-dimethyloctanol	9 ± 1
(±)-β-citronellol	8 ± 1
heptanol	7 ± 1
cis-4-heptenol	0
(±)-linalool	0

Supplementary Table 4. Relative conversion rates for IO substrates.

Values are the average of 3 replicates ± standard error. The different substrates (100 µM) were incubated for 5 minutes at 27 °C with 0.25 µM iridoid oxidase. Ethyl acetate extracts were analyzed by GC-MS (see Methods). Activity was quantified based on peak area of products. Minor conversion of linalool, 8-oxogeraniol and 8-oxogeranial was observed using higher enzyme concentrations.

Compound	relative conversion rate (%)
iridotrial	100 ± 5
(+)-β-citronellol	20 ± 4.5
nerol	2 ± 0.5
lavandulol	2.5 ± 0.5
linalool (mix of isomers)	0
8-oxogeraniol	0
8-oxogeranial	0
geraniol	0
7-deoxyloganic acid	0

Supplementary Reference

1 Omura, T. & Sato, R. The carbon monoxide-binding pigment of liver microsomes. i. evidence for its hemoprotein nature. *J. Biol. Chem.* **239**, 2370-2378 (1964).